Catching Whales and Minnows using WiFiNet: Deconstructing Non-WiFi Interference using WiFi Hardware

Technical Report 2011, Department of Computer Sciences, UW Madison

Shravan Rayanchu, Ashish Patro, Suman Banerjee
University of Wisconsin Madison

Abstract

We present WiFiNet— a system to detect, localize, and quantify the interference impact of various non-WiFi interference sources on WiFi traffic using commodity WiFi hardware alone. While there are numerous specialized solutions today that can *detect* the presence of non-WiFi devices in the unlicensed spectrum, the unique aspects of WiFiNet are four-fold: First, WiFiNet quantifies the actual interference impact of each non-WiFi device on specific WLAN traffic in real-time, which can vary from being a *whale* — a device that currently causes a significant reduction in WiFi throughput — to being a *minnow* — a device that currently has minimal impact. WiFiNet continuously monitors changes in a device's impact that depend on many spatio-temporal factors. Second, it can accurately discern an individual device's impact in presence of multiple and simultaneously operating non-WiFi devices, even if the devices are of the exact same type. Third, it can pin-point the location of these non-WiFi interference sources in the physical space. Finally, and most importantly, WiFiNet meets all these objectives not by using sophisticated and high resolution spectrum sensors, but by using emerging off-the-shelf WiFi cards that provide coarse-grained energy samples per sub-carrier. Our deployment and evaluation of WiFiNet demonstrates its high accuracy — interference estimates are within $\pm 10\%$ of the ground truth and the median localization error is ≤ 4 meters. We believe a system such as WiFiNet can empower existing WiFi clients and APs to adapt against non-WiFi interference in ways that have not been possible before.

1 Introduction

WiFi devices share the unlicensed spectrum with a plethora of other devices and technologies. A few examples include Bluetooth headsets, ZigBee devices, cordless phones, various game controllers (Xbox, Wii, etc.), and custom wireless security camera systems. Even non-communicating appliances such as microwave ovens, leak energy into this spectrum. Each such device can cause interference to WiFi communication. Since WiFi's constituent standard (IEEE 802.11) does not have any explicit mechanism to recognize such non-WiFi sources of interference, typical WiFi links have no reasonable way to guard against such interference. In this paper, we design a *WiFiNet* — a collaborative neighborhood of WiFi nodes — to "catch" various non-WiFi transmitters causing harmful interference to WiFi communication (Figure 1). More specifically, through WiFiNet we can answer the following questions — *how much* interference is any non-WiFi RF transmitter (e.g., a Bluetooth headset, an active analog phone, or a microwave oven) causing to an existing WiFi communication and *where* in the physical space is each such non-WiFi interferer located?

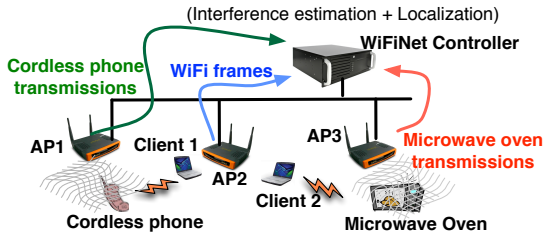

Figure 1: Illustration of WiFiNet's architecture.

Much of the prior work has employed custom hardware to tackle non-WiFi interference. Examples include commercial products such as AirMaestro [1] and Wispy [4] that build specific signatures to *detect* the presence of a device. Recent research efforts (e.g., RFDump [13], DOF [8], TIMO [18]) have used the flexibility allowed by software radios to develop novel signal processing techniques and physical layer designs to co-exist with these devices. The unique aspect of WiFiNet is that it is built entirely on top of standard WiFi network interface cards (NICs). In particular, an emerging class of WiFi NICs, such as those based on the Atheros 9280 chipset, as part of their WiFi frame decoding process, provide coarse-grained energy samples per sub-carrier of a WiFi channel. These energy samples are a few orders of magnitude lower in resolution than available to the sophisticated spectrum analysis tools. In our recent work Airshark [16], we have shown that even with such a low resolution system, a regular WiFi node (either an Access Point or a client) can individually *detect* the presence of non-WiFi devices.

Airshark is, however, is only the first step in the broad space of deconstructing non-WiFi interference and quantifying their impact on WiFi links. WiFiNet leverages collaboration between multiple WiFi nodes to address both quantification of interference impact and localization of these interferers, as we explain below.

Quantifying non-WiFi interference impact in real-time: The mere presence of a non-WiFi device, as detected by Airshark, in the vicinity of a WiFi transmitter is not always harmful. For instance, an active analog cordless phone at a specific location, may only have a minimal impact on a particular WiFi link. We call such a low-

impact non-WiFi device, a *minnow*. On the other hand, a microwave oven radiating a significant amount of energy in its vicinity might cause severe disruption to nearby WiFi links. We call such an interferer, a *whale*.

However, the impact of interference from the same non-WiFi device can quickly change over time. For instance, if the microwave oven's setting is adjusted to operate with a low power level, this device may suddenly turn into a minnow. On the other hand, if the cordless phone user moves to a different location which is closer to the WiFi link, this device might turn into a whale with respect to this WiFi link. It is even possible that the impact of the cordless phone on the WiFi link changes due to properties of the WiFi link itself. For example, when the WiFi link is operating at 54 Mbps, the disruptive impact of the cordless phone is quite high, with the impact decreasing as a rate adaptation algorithm reduces the WiFi link's choice of PHY rates. WiFiNet tracks this continuously changing impact of non-WiFi transmitters on WiFi communication in real-time, adjusting its interference estimates immediately as operating parameters change (e.g., the microwave power setting is changed, or the WiFi device's PHY rate selection algorithm starts operating with a higher rate).

Locating non-WiFi interferers: WiFiNet also determines the physical location of such non-WiFi transmitters immediately, so that the precise source of such interference can be determined, and if needed, such interfering devices can either be re-configured or disabled.

Through these new and unique capabilities, WiFiNet provides new RF management tools for WiFi environments using off-the-shelf WiFi NICs only, obviating the need for sophisticated wireless hardware. In fact, WiFiNet can be easily implemented and integrated into enterprise WiFi APs to achieve improved mitigation strategies against non-WiFi interference for enterprise environments.

1.1 Challenges in designing WiFiNet

In designing and implementing the capabilities of WiFiNet, we had to overcome the following set of challenges:

How to detect multiple devices of the same type? In many wireless environments, there are multiple devices of a given type, e.g., two different cordless phones. It is possible that among these two phones, one is a whale and causes 80% loss in throughput to a WiFi link, while the other is a minnow and causes only 5% loss in throughput. To differentiate between these two interferers, WiFiNet needs to determine how many devices of each type are operating at any given instant. To achieve this goal, WiFiNet utilizes tight clock synchronization, and employs signal clustering techniques operating on some device specific attributes (when available) and signal strength observations gathered by multiple WiFi detectors to identify the unique transmission contributions from different, potentially identical, non-WiFi devices. Our prior work, Airshark, builds signatures of each device type to detect the presence of any such device in the vicinity of the detecting WiFi node. But such an individual WiFi node is not able to determine if there is only one or two or three different FHSS cordless phones in the vicinity, and hence, cannot attribute which part of wireless transmissions belong to which such interferer.

How to estimate each device's impact? After segregating each non-WiFi device's transmissions, WiFiNet uses specific timing analysis for estimating the impact of each interferer — time-frequency overlaps between the WiFi frames and non-WiFi device's transmissions are analyzed and correlated with the outcomes (frame success or loss) to discern the impact of each device. Our technique works well for both low and high duty devices. In our design, we take into account the carrier sensing interference, interference from WiFi sources and multiple PHY rates of operation used by WiFi links.

How do we localize the non-WiFi device? Localization in indoor wireless environments is a well studied problem [5, 6, 19, 22]. Common techniques include signal strength based triangulation [22] and RF fingerprinting approaches [5]. However, the key requirement for such localization approaches is for multiple detectors to *detect the same transmission* at different signal strengths. In the commonly known WiFi localization techniques, this is easy because the different detectors decode the same wireless frame and use the frame's identity to ensure sameness.

In our case, the WiFi detectors cannot decode the non-WiFi transmissions, and hence cannot immediately assign the same identity to "pulses" received from the non-WiFi transmitters. A core challenge that we needed to solve is for different WiFi detectors to determine which received pulses correspond to a single transmission from the same non-WiFi device. The next challenge is to build a model for localization. Propagation characteristics are similar for both WiFi and non-WiFi transmitters since they operate on the same frequency. WiFiNet exploits this fact and builds the model by exchanging WiFi frames and recording signal strength measurements. Since the transmit power of non-WiFi devices can be arbitrarily different from that of WiFi nodes, the model takes this into account by operating on the *difference* in received signal strengths. Through experiments, we show the feasibility of this approach for non-WiFi device localization using WiFi-only detectors.

Summary of key contributions: Summarizing, the key contributions of our WiFiNet system are three-fold: (i) it detects and discerns the transmission contributions of different non-WiFi interferers in the vicinity of the WiFi detectors; (ii) it attributes interference impact of each such non-WiFi device for any given WiFi link, classifying them as whales, minnows, or anything else in between, through collaborative observations; and (iii) it pinpoints the location of each such non-WiFi interferer so that they can

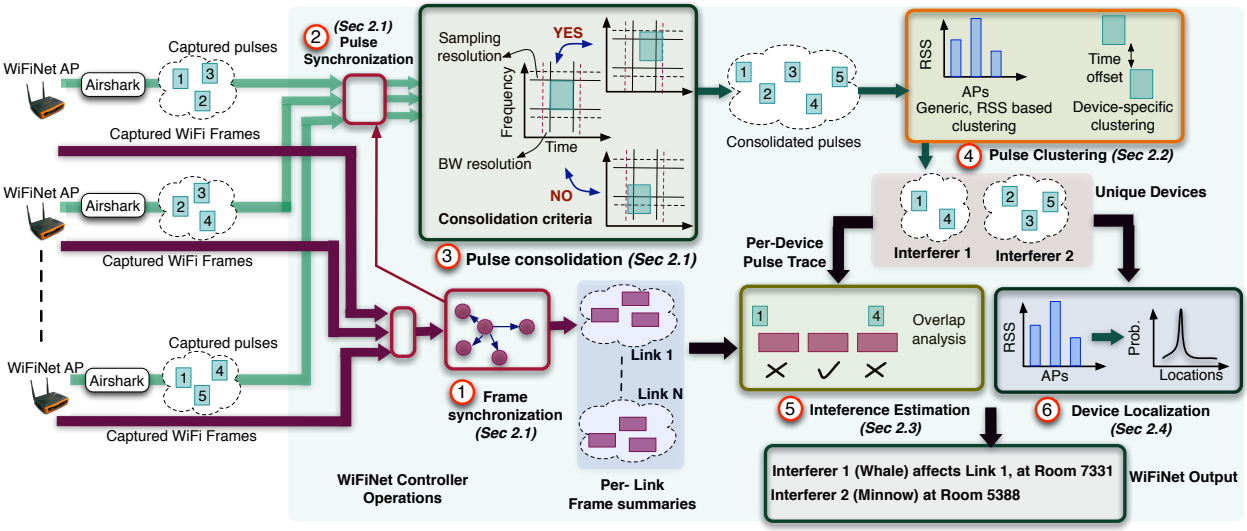

Figure 2: Flow of operations in WiFiNet. WiFiNet **APs capture spectral samples as well as WiFi frames. Each AP runs** Airshark **[16] to detect non-WiFi devices and output non-WiFi pulses (transmissions) tagged with device type. WiFi frames are used to synchronize the clocks at the APs. Synchronized clocks at the APs are then used to consolidate the pulses across multiple APs using a heuristic (§2.1). Consolidated pulses are then clustered using (i) RSS based clustering and (ii) device-specific clustering methods to output unique non-WiFi device instances and their pulses (§2.2). For each non-WiFi device instance and WiFi link, the interference detection module then analyzes the impact of the device on the link using transmission overlaps (§2.3). Model-based localization algorithms are used to localize each non-WiFi device instance (§2.4).**

be independently re-configured or disabled. All of these capabilities are implemented using WiFi-only detectors.

The entire WiFiNet system has been implemented using the Atheros AR 9280 based WiFi NICs, and evaluated in detail through various experiments. Our results indicate a typical impact determination accuracy of $> 90\%$ and a localization error of < 4 meters in these environments.

2 WiFiNet

We start by presenting an overview of WiFiNet's architecture, followed by the details of its design and operation.

Architecture and flow of operations. WiFiNet employs collaborative observations from multiple WiFi-only detectors spread across a network to perform its non-WiFi device interference estimation and localization operations. Since most enterprise APs today come equipped with multiple WiFi radios, one way to deploy WiFiNet would be to employ one of the radios as a detector. In such a setting, WiFiNet can function as follows. All the enterprise APs are connected to a central controller over an Ethernet backplane. Each AP has two radios: (i) a regular radio that used to communicate with the clients, and (ii) a detector radio that continuously captures spectral samples as well as WiFi frames. APs run Airshark [16] to process the spectral samples and perform device detection. Airshark outputs a set of "pulses" (time-frequency blocks representing non-WiFi device transmissions), and tags these pulses with the appropriate device type (e.g., Bluetooth, ZigBee, etc.). Each pulse reported by Airshark consists of the start and end timestamps, center frequency and bandwidth of the pulse, the average received power of the pulse, and a tag that indicates the device type. Next, the APs also process the captured WiFi frames to create a per-client frame transmission summary: frame start and end timestamps, PHY rate, and reception status (*i.e.*, whether the AP received an ACK for this frame or not). The proximity between the two radios ensures that the detector radio receives the majority of frames transmitted by the regular radio due to capture effect, thereby creating an accurate summary of frame transmissions [20]. The per-client WiFi frame transmission summaries and the captured non-WiFi pulse traces are forwarded to controller to identify the individual non-WiFi device instances, estimate their interference impact and localize them. Figure 2 presents the overall control flow. We now explain each of these tasks in detail.

2.1 Identifying unique pulses

Since the same pulse can be received by multiple APs in the WLAN, the first task for the controller is to consolidate the traces and identify the *unique pulses* transmitted by different non-WiFi devices operating in the environment. To do this, the controller has to identify the "common" pulses received by the APs and create a single consolidated pulse. However, finding common pulses is not straightforward as WiFi APs *cannot decode* non-WiFi pulses.

Pulse consolidation. WiFiNet uses a heuristic to consolidate the pulses: if two APs receive a pulse that has the same device type (e.g., Bluetooth), has the same start and end times, has the same center frequency and bandwidth, then most likely the APs received the same pulse (transmitted by a particular non-WiFi device). In practice, we allow a certain leeway as these parameters might not exactly match e.g., we allow the maximum difference between the pulse start (and end) times to be FFT sampling resolution of the WiFi card (116μs for AR9280 card) and that between pulse center frequencies (and bandwidths) to be resolution bandwidth of the WiFi card (312.5 kHz or equal to 802.11 sub-carrier spacing).

To apply the heuristic, however, would require the pulse traces at the APs to be synchronized. How do we synchronize the pulse traces without knowing common pulses (*i.e.*, reference points)? WiFiNet solves this issue by leveraging the WiFi hardware — the timestamps of the pulses are derived from the *same clock* that is used to timestamp the captured WiFi frames. WiFiNet first synchronizes the clocks at all the APs using captured "common" frames as reference points, and then uses the synchronized APs to find "common" pulses. We now explain these tasks.

Opportunistic synchronization. Synchronization can be easily carried out if we find one reference frame that is received by all WiFiNet APs in the WLAN. However, this is highly unlikely in practice as the wireless signal attenuates over distance. Therefore, WiFiNet *opportunistically synchronizes* 'pairs of APs' using common received frames (reference frames used for synchronization are typically beacon frames or data frames without the retransmit bit set [21, 15]) , and then *transitively* synchronizes the sniffer radios at all the APs using a graph based approach:

1. Instantiate a synchronization graph, $syncGraph = (S, E)$ where each vertex s_i represents the sniffer radio at WiFiNet AP i, and the weight $w(e_{ij})$ of the edge $e_{ij} : s_i \rightarrow s_j$ represents the clock skew between the APs. Initially, S comprises of all vertices and has no edges.
2. For each pair of WiFiNet APs (s_i, s_j), we start by finding the set of reference frames (common received frames). Compute difference in timestamps for each of the reference frames, and use the median value as the clock skew. This results in instantiating an edge e_{ij} in the *syncGraph* with weight equal to skew between the APs.
3. After processing all pairs of APs, start with a reference AP (s_0), chosen randomly, and perform a *breadth-first search* on the *syncGraph* to transitively synchronize all the APs with respect to the reference AP.

The above synchronization procedure is repeated every *sync interval* in order to account for the clock drift.

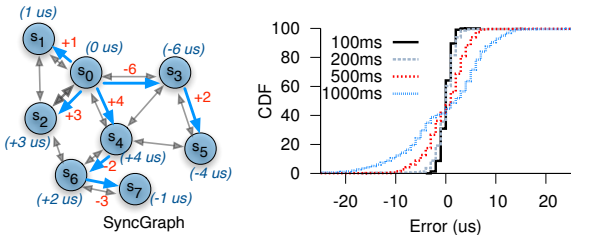

Figure 3: (left) Illustration of graph based opportunistic synchronization used in WiFiNet. Each node is an WiFiNet AP (s_0 is the reference AP), weights on the edges correspond to the pair-wise AP skews, and the numbers in the parentheses are the final synchronization offsets of the APs (*i.e.*, skews w.r.t. reference s_0) (right) CDF of synchronization error for our deployment of 8 WiFiNet APs at different sync intervals. Error in synchronization is ≤ 6 μs for a sync interval of 500 ms.

Figure 3 shows the synchronization error as a function of sync interval for our deployment of 8 WiFiNet APs. We observe that the error increases with the increase in sync interval (e.g., an error of < 6 μs for an interval of 500 ms). In WiFiNet, we use a sync interval of 100 ms which results in tight synchronization between the APs (an error of less than $2-4$ μs in most cases).

Output from consolidation. The controller applies the appropriate synchronization offsets to each AP's pulse trace and then finds the common pulses among the APs using the heuristic mentioned above. The consolidation process can be carried out efficiently as the pulses are sorted by time. After consolidation, the controller is left with unique pulses transmitted by non-WiFi devices, and for each unique pulse, we associate an RSS vector $\mathbf{r} = [r_0, \ldots, r_{N-1}]$ that represents the received power of this pulse at each of the N APs in the WLAN. We set r_i to the average received power of the pulse at ith AP, if the pulse was indeed received this AP, otherwise $r_i = \phi$.

2.2 Identifying unique device instances

After obtaining the unique pulses, the next task for the controller is to detect the number of non-WiFi device instances, segregate the pulses belonging to each instance and establish a unique ID for it. WiFiNet first segregates the pulses according to their device type, and employs *clustering algorithms* for further segregation. The algorithms determine "the number of clusters" (non-WiFi device instances), and assign each pulse to a cluster. The combination of (device type, cluster center) is then used as the ID for this device instance. In our current prototype, we implement (i) a generic, RSS based clustering that is applicable to all non-WiFi devices and (ii) clustering based on timing properties that is specific to some non-WiFi device types. We now explain both approaches.

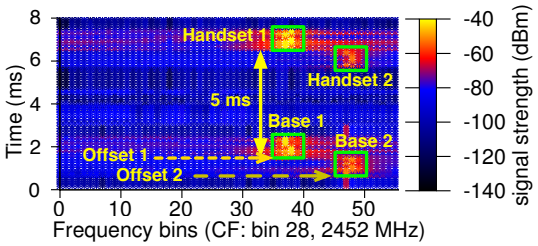

Figure 4: Heatmap of 4 FHSS cordless phone devices (2 base/handset pairs) captured by a WiFiNet AP, showing the timing property. Each base/handset pair emits two short pulses that are both at the same center frequency and are separated by 5 ms. The pair then jumps to a different center frequency after 10 ms and repeats the process. WiFiNet identifies the pulses belonging to each device by calculating their timing offsets (pulse start time modulo 10 ms).

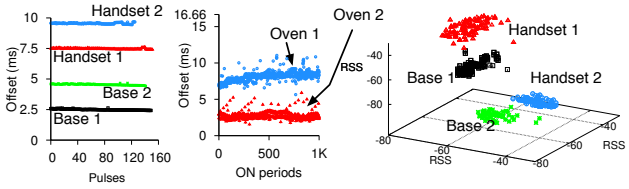

Figure 5: Segregating pulses in the presence of multiple, simultaneously operating devices of the *same type*, based on WiFiNet's device specific and generic clustering. Figure shows clusters of pulses from (left) 2 FHSS cordless phone base/handset pairs (4 FHSS cordless devices) using pulse start time offset (middle) 2 Microwave ovens using ON-period offset (right) 4 FHSS cordless devices using a generic, RSS based k-means + EM-clustering technique using 3 WiFiNet APs.

2.2.1 Generic clustering based on signal strength

WiFiNet's generic clustering approach operates on RSS vectors that are N-dimensional (*i.e.*, vector sizes grow with the number of APs). Since the performance of clustering mechanisms typically degrades with increase in the number of dimensions, we first filter out some of the dimensions before performing clustering.

Reducing vector dimensions. We use some optimizations to reduce the number of dimensions: (i) clustering is performed every *scan window* (5 secs in our current prototype) to keep the number of pulses low (ii) APs not receiving any pulse in the current window are discarded (iii) The controller uses the *syncGraph* (§2.1) as a proxy for "RF neighborhood" of APs and segregates the APs into different partitions using the following heuristic. For each pulse, we determine the WiFiNet AP with the highest RSS, and increment a counter for this AP. After processing all the pulses, we assign the AP with the highest counter to first partition. We then pick each AP (in the decreasing order of the counters) and place it in one of the existing partitions if it satisfies the RF neighborhood constraint: in the *syncGraph*, the AP has to be within a 2-hop neighborhood of the AP with the highest counter for this partition, otherwise we create a new partition for this AP. This breaks the clustering problem into sub-problems, each operating on one partition.

Handling missing values. After partitioning the RSS vectors to reduce the dimensionality, another problem remains: RSS vectors might still have missing values (*i.e.*, $r_i = \phi$) for some columns. This is because APs might capture pulses intermittently (i) as they are far from the device, or (ii) due to a stronger signal from other WiFi or non-WiFi transmissions [16] that overlapped with the pulse. While it is possible to define a distance function for clustering that ignores missing values in the vectors, such a function is unsuitable for many traditional clustering algorithms as it doesn't satisfy certain mathematical properties such as the triangle inequality [10]. This presents us with two choices, (i) use clustering algorithms which allow a certain degree of freedom in the formulation of a suitable distance function or (ii) fill in the missing values using a best-effort approach, and then use traditional clustering algorithms. We explored both these choices.

(Method 1) Density-based clustering. We used DBSCAN [12], a density-based clustering approach that allowed us to formulate a distance metric that can handle missing values. Let P and Q be the set of APs receiving the pulses p and q, and C be the set of common APs that received both pulses. We define $\eta = |C|/\max(|P|, |Q|)$ and compute the distance between two pulses p and q as:

$$\tau(p,q) = \begin{cases} \sqrt{\frac{1}{|C|}\sum_{i \in C}\left[r_i^{(p)} - r_i^{(q)}\right]^2} & \text{if } \eta \geq \eta_o, |C| \geq C_{min} \\ +\infty & \text{otherwise} \end{cases}$$

The above measure only takes signal strength from common APs into account, and any missing RSS values do not affect the distance. Intuitively, the introduction of parameters η_o and C_{min} is to account for the case when the difference in the set of APs receiving the pulses is too large. We comment on these parameters in §3.

(Method 2) k-Means + EM-clustering. Another approach to handle missing values is to first perform *imputation* — missing values in a particular column are replaced (e.g., using a median or mode of the column). In WiFiNet, we use *EM-Imputation* [3], a well known imputation method, where the missing values are replaced by using expectation maximization with a multi-variate normal model. After imputation, we can use traditional clustering mechanisms as the distance function (e.g., Euclidean) can now operate on all the columns of the vectors. We experimented with several clustering algorithms and found that a combination of k-Means and EM-clustering perform the best: WiFiNet controller iteratively runs the k-Means clustering algorithm with different values of k ($1 \leq k \leq k_{max}$), and then picks the best solution [3].

This is used as the initial solution to the EM-clustering algorithm, which outputs the final non-WiFi device instances and the corresponding pulses. In our experiments, we set $k_{max} = 10$ *i.e.*, we assume that the maximum number of *simultaneously operating* devices of the *same type* to be 10. Figure 5 (right) shows an example result for RSS based clustering for 4 FHSS cordless phone device instance using 3 WiFiNet APs. In §3, we compare the performance of the above clustering algorithms.

2.2.2 Clustering based on device specific attributes

We found that some non-WiFi device types exhibit certain specific timing properties that can be exploited to provide better clustering performance compared to the generic RSS based clustering approach. In WiFiNet, we implemented such clustering for two non-WiFi device types:

— *Pulse start time offset for FHSS cordless phones.* WDCT cordless phone sets cycle through frames of 10 ms: each frame consists of two short pulses, one emitted by the base at the beginning of the frame and the other by the handset, occurring after 5 ms (both at the same center frequency). Both base and handset then jump to a different center frequency for the next frame. Figure 4 shows the pulses from two cordless phone sets (*i.e.*, 2 base/handset pairs, a total of 4 unique cordless phone devices) captured by WiFiNet. Figure 5 (left) shows that clustering based on the pulse start time offsets (t MOD 10) can segregate the pulses belonging to each device.

— *ON-period offset for microwave ovens.* Microwave ovens emissions exhibit an ON-OFF pattern, typically periodic with a frequency of 60 Hz (frequency of the AC supply line) *i.e.*, a period of 16.66 ms [16]. WiFiNet computes the offset for start times of the microwave pulses (ON periods) as t MOD 16.66 and uses this to segregate their pulses. Figure 5 (middle) shows the result of clustering pulses from two microwave ovens operating simultaneously.

2.3 Interference Estimation

After clustering, WiFiNet controller now has a set of clusters, each representing a unique non-WiFi device instance. We now explain how the controller can analyze the interference impact of each device instance.

Intuition and Overview. For each non-WiFi interferer instance and a WiFi link, WiFiNet controller performs interference analysis by correlating the the link's frame transmission with the non-WiFi device's pulse transmissions and observing the reception status of the frames. It measures the impact of a non-WiFi device on a WiFi link by computing the probability of a frame loss when the frame overlaps with a simultaneous transmission from the non-WiFi device. Intuitively, the extent of interference is directly proportional to the probability of losing overlapping frames. This allows WiFiNet to maintain a

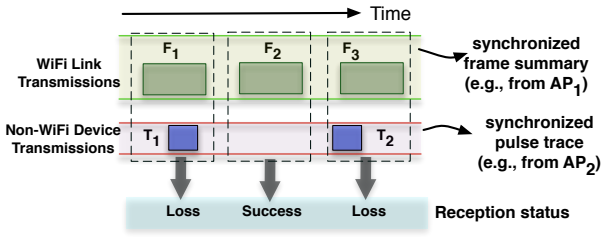

Figure 6: Illustration of interference estimation in WiFiNet.

continuous interference model, where the extent of interference can be any value between 0 and 1. For instance, in Figure 6, the controller observes that frames transmitted on a link are *unsuccessful* whenever a non-WiFi device's *pulse overlaps with the frame in time (and frequency) i.e.*, frames F_1 and F_3 overlap with non-WiFi device pulses T_1 and T_2, and are lost. It can therefore infer that the device strongly interferes with the link. Such fine-grained timing analysis is possible because APs are tightly synchronized (§2.1) and they use the *same clock* to timestamp both pulses and the frames. We now explain our interference estimation metrics.

Metrics for interference estimation. Formally, the interference estimation metrics used in WiFiNet can be explained as follows. Let I be the event that interference from a particular non-WiFi device causes a frame transmission to be unsuccessful. Let L be the event of an unsuccessful transmission due to background losses (e.g., due to weak signal) and O denote the event of an overlap between the frame transmission and a simultaneous transmission (e.g., a pulse) from the non-WiFi interferer.

— *(Metric 1) Impact given overlap.* Conditional probability, $p[I|O]$ is used to measure the *impact given overlap i.e.*, probability that a frame is unsuccessful given an overlap with a simultaneous transmission from a non-WiFi device.

— *(Metric 2) Overall impact.* WiFiNet also maintains $p[I]$, the *overall impact* of a non-WiFi device. Here, $p[I]$ is equal to $p[I|O]{\cdot}p[O]$ (when there is no overlap, $p[I|\neg O]$ is simply 0). That is, $p[I]$ is probability of frame loss due to the overall activity from the non-WiFi device.

We note that $p[I]$, the overall impact of the interferer, depends on the probability of overlap $p[O]$, which varies based on the link and interferer transmission patterns. Whereas, $p[I|O]$ is *not affected* by these transmission patterns *i.e.*, $p[I|O]$ indicates the *worst case impact* of the interferer on the link, which is observed when $p[O]{=}1$ (*i.e.*, when the transmissions of link and the interferer always happen to overlap). Next, we explain how these probabilities are estimated by WiFiNet in real-time.

Interference estimation. The controller measures the total number of frames transmitted (n) on the WiFi link of interest, the number of frames that overlapped with the

non-WiFi device's transmissions (n_o) and n_o^l, the number of overlapped frames that were unsuccessful. It then computes $p[O]$, the probability of transmission overlap as n_o/n. Next, the controller computes $p[(I \cup L)|O] = n_o^l/n_o$ *i.e.*, the probability of an unsuccessful frame transmission due to either background losses or interference from the non-WiFi device, given an overlap in transmissions. It also computes the probability of frame loss when there is no overlap from the interferer, $p[L]$ as n_{no}^l/n_{no}. Here, $n_{no} = n - n_o$ is the number of frames without overlap and n_{no}^l is the number of n_{no} transmissions lost. Since L is independent of O, we have $p[L|O] = p[L|\neg O] = p[L]$. Also, I and L are independent events, and so we have $p[(I \cup L)|O] = p[I|O] + p[L] - p[I|O] \cdot p[L]$. That is,

$$p^{\text{WiFiNet}} = p[I|O] = \frac{\Big(p[(I \cup L)|O] - p[L]\Big)}{(1 - p[L])} \quad (1)$$

Using $p[(I \cup L)|O]$ and $p(L)$, WiFiNet controller estimates $p[I|O]$. Following this, the controller also computes the overall interference $p[I]$ as $p[I|O] \cdot p[O]$.

Handling overlaps from multiple non-WiFi interferers. In general, a frame transmission may overlap with multiple simultaneous transmissions from potential non-WiFi interferers. In this case, WiFiNet controller attributes the frame transmission success or loss to each overlapping non-WiFi interferer. We observed that *diversity* in the frame transmission times [20] as well as the diversity in transmission times of different non-WiFi devices allows WiFiNet to distinguish the *true* non-WiFi interferer from the other *false* non-WiFi interferers (*i.e.*, devices that happened to transmit at the same time as the true interferers). In particular, such a diversity allows WiFiNet to observe further transmissions from false non-WiFi interferers that overlap with the frames but do not lead to a frame loss. In our experience, such a transmission diversity arises due to (i) distinct transmission characteristics of different non-WiFi devices (e.g., frequency hopping devices typically emit short pulses at different center frequencies) and (ii) diversity in the usage times of non-WiFi devices [16], where in a typical enterprise not more than $3-4$ devices were found to be *simultaneously active*.

2.3.1 Enhancements to the basic technique

Handling high duty devices operating with other devices. Transmissions from multiple devices that *always* happen to overlap in time can lead to cases where WiFiNet can make incorrect estimates. For example, WiFiNet may identify a false interferer as a true interferer if the transmissions from the false interferer always happen to overlap with that of a true interferer. In our experiments, we found that such a scenario is unlikely when using pulsed transmitters (e.g., ZigBee devices) or frequency hopping devices (e.g., Bluetooth or FHSS cordless phones) that typically emit short pulses. However, operating high duty devices (e.g., analog cordless phones) that *continuously* emit energy alongside other non-WiFi devices will cause their transmissions to always overlap that can lead to incorrect estimates (§3.1.4).

We use two refinements to the basic approach to correctly identify interference impact of a non-WiFi interferer W operating alongside a high duty device H: (i) when computing $p[I_H|O_H]$ for a high duty device, we only consider the frames that *do not overlap* with a transmission from any other non-WiFi device. Here, $p[O_H] = 1$ and $p[I_H|O_H] = p[I_H]$ and (ii) we modify Equation 1 to compute the estimate $p[I_W|O_W]$ of a non-WiFi device W when it operates alongside a high duty device H as

$$p[I_W|O_W] = \frac{\Big(p[(I_H \cup I_W \cup L)|O_W] - p[I_H \cup L]\Big)}{\Big(1 - p[I_H \cup L]\Big)} \quad (2)$$

Here, $p[(I_H \cup I_W \cup L)|O_W]$ can be computed by measuring the losses that happen when the frames overlap with transmissions from non-WiFi device W (as well as those from the high duty device H). Now, knowing $p(I_H)$ and $p(L)$, we can compute $p[I_W|O_W]$. While such an approach can handle most cases, it cannot handle pathological cases where two high duty devices are activated at the exact same time — since both the devices continuously emit energy, nothing useful can be said about the impact of each device (§3.4.4). If however, the interference impact of one of the devices is known, then that of the other can be computed using the above formulation. As we show later in §3, typically, diversity in transmission times of non-WiFi devices, coupled with the above refinements allows WiFiNet to correctly identify the true non-WiFi interferer in realistic wireless settings.

Quantifying impact at different 802.11 rates. The impact of a non-WiFi interferer on a WiFi link also depends on the PHY rate being used by the WiFi transmitter. To account for this, WiFiNet controller records the overlaps and losses separately for each different PHY rate, and computes a separate interference estimate for each rate. This helps quickly the estimate interference impact at each PHY rate when using dynamic bit rate adaptation as opposed to high-overhead bandwidth tests that require controlled experiments at each PHY rate to estimate the same [20].

Handling sender-side interference. Similar to the procedure used for interference analysis, WiFiNet controller can infer whether a WiFi transmitter is deferring to a non-WiFi device by correlating the WiFi frame transmissions with

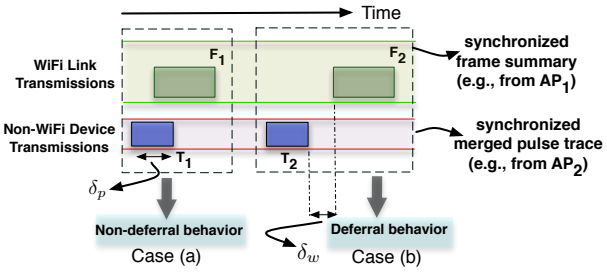

Figure 7: Illustration of carrier sensing estimation in WiFiNet**.**

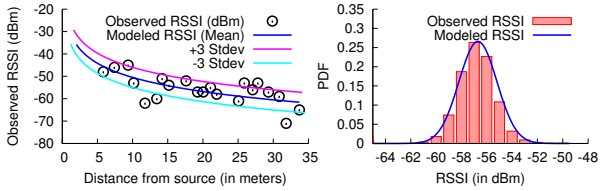

Figure 8: (left) Path loss model created by a WiFiNet **APs using WiFi transmissions (right) PDF of actual RSSIs observed at a sample location and the model created using a normal distribution.**

the non-WiFi pulse transmissions. Figure 7 shows two cases of interest. Case(a) when the WiFi transmitter is not deferring to the non-WiFi device, WiFiNet controller will observe several instances where the frame transmission *starts while the pulse transmission is in progress*. Case(b) When the WiFi transmitter is indeed deferring to the non-WiFi device, WiFiNet controller will not observe instances where frame transmission starts while the pulse transmission is in progress. However, this condition alone is not enough to infer that the WiFi transmitter is deferring to the non-WiFi device, as it may happen that the WiFi transmitter did not have any packets to send while the pulse transmission was in progress *i.e.*, the WiFi transmitter did not contend for the medium. To identify the deferral instances, we use a heuristic similar to the prior work on carrier sense estimation between WiFi links [15, 20]: the controller identifies the deferring frames as those where the difference between the pulse transmission end time and the frame transmission start time is within a certain threshold δ_w. Here, δ_w is the maximum time spent by the WiFi transmitter performing back-off and is set to $28+320$ μs (DIFS + Max back-off period for 802.11g).

The controller can now compute the fraction $\Delta_{cs} = \frac{n_d}{n_d+n_{nd}}$ where n_{nd} is the number of Case (a) instances that indicate *non-deferral* behavior and n_d is the number of Case (b) instances that indicate *deferral* behavior. If the transmitter is indeed deferring, Δ_{cs} would be close to 1. Whereas, if the transmitter is not deferring to the non-WiFi device, the difference in the pulse and frame start transmission times would be uniformly distributed in the interval $[0, \delta_p + \delta_w]$, where δ_p is the duration of the pulse. That is, we expect $\Delta_{cs} \approx \frac{\delta_w}{\delta_p+\delta_w}$. Typically, $\delta_p > \delta_w$, therefore Δ_{cs} is low for cases of non-deferral (e.g., for δ_p for microwave ovens, cordless phones, and Bluetooth devices is 8 ms, 1.25 ms, and 625 μs respectively). In our experiments, using a threshold of $\Delta_{cs} > 0.8$ was able to correctly identify deferring WiFi transmitters (§3.4.2).

Extensions to handle WiFi interference. In general, WiFi links can also experience interference from other WiFi links. We extend our basic approach to measure the overlaps between frame transmissions on a particular WiFi link and the frame transmissions on other WiFi links to compute the probability of frame loss due to hidden interference [20]. In §3.1.5, we experiment with non-WiFi interferers operating alongside hidden terminals and show that WiFiNet is correctly able to identify the true interferer.

Interactions with external interference. External interference can be caused by non-WiFi devices that are not a part of the enterprise or by other non-enterprise wireless traffic (e.g., traffic from nearby WiFi networks). In both these cases, interference estimation can proceed as is if at least one of the APs is able to capture the pulse (or frame) transmissions from the interference source. However, if the transmissions from the non-WiFi device (or the external WiFi transmitter) are not captured by any WiFiNet AP, then WiFiNet controller would not be able to identify the source of interference.

2.4 Localizing a non-WiFi device instance

WiFiNet uses a computationally efficient, real-time localization scheme that imposes *zero* profiling overhead, and physically locates the non-WiFi device instance of *unknown transmit power* using a modeling based approach. Below, we explain our localization models.

2.4.1 Model-based localization

Let $\hat{\mathbf{r}} = [\hat{r}_0, \ldots, \hat{r}_{N-1}]$ be the mean RSS vector of all the pulses present in the cluster assigned to a non-WiFi device instance. For localization, we only consider the APs with valid received powers (*i.e.*, $\hat{r}_i \neq \phi$). We divide the entire region into grids of size 0.25×0.25 meters. Let i denote the grid location of AP_i. Let d_{ij} denote the distance between grids i and j. Let $P(l|\hat{\mathbf{r}})$ denote the probability of the non-WiFi device being at location l, given that the received power vector is $\hat{\mathbf{r}}$. We wish to determine the grid location l such that $P(l|\hat{\mathbf{r}})$ is maximized *i.e.*, we want $\text{argmax}_l P(l|\hat{\mathbf{r}})$. Using Bayes' theorem, $P(l|\hat{\mathbf{r}})$ can be written as $P(\hat{\mathbf{r}}|l).P(l)/P(\hat{\mathbf{r}})$. Assuming all locations are equi-probable, and since $P(\hat{\mathbf{r}})$ is constant for all l, we have $\text{argmax}_l P(l|\hat{\mathbf{r}}) = \text{argmax}_l P(\hat{\mathbf{r}}|l)$, which can be calculated as $\text{argmax}_l \prod_{i=1}^{N-1} P(\hat{r}_i|l)$ (assuming independence [22]). Put another way, the grid location l where the non-WiFi device is most likely present can be computed using,

$$\text{argmax}_l \sum_{i=1}^{N-1} \log P(\hat{r}_i|l) \quad (3)$$

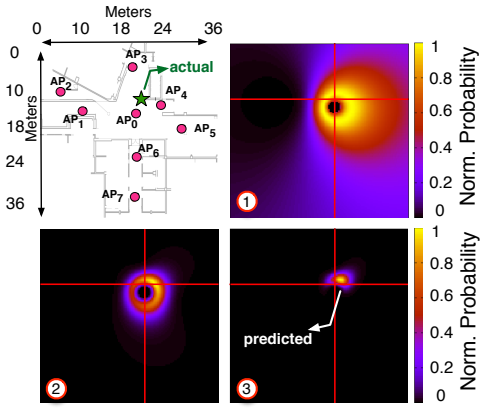

Figure 9: (top, left) Deployment 1 comprising 8 APs. (rest of the sub-figures) FHSS cordless phone device is placed at the starred location. Grid probabilities for predicted phone locations after processing 1, 6 and all AP pairs when using Model-UTP algorithm.

Case of known transmit power (Model-TP). If the non-WiFi device instance is at a grid l, then the *expected* received power at AP_i (located at grid i) can be modeled as a normal distribution $\mathcal{N}(\mu_{il}, \sigma^2)$, where σ is the shadowing variable, and μ_{il} is the *expected mean* of the received power that can be modeled as $\mu_{il} = R^o - 10\gamma log_{10} d_{il}$. Here, γ is the pathloss exponent and R^o is the power received from the non-WiFi device when placed at a distance of 1 meter from an AP (referred to as *transmit power*). How can we estimate γ for the non-WiFi device? WiFiNet APs derive γ using *WiFi frames i.e.*, each WiFiNet AP uses the data packets or beacons transmitted by neighboring WiFiNet APs to model the propagation loss characteristics (Figure 8) — since both WiFi devices and non-WiFi devices operate on the frequency, the propagation loss characteristics of their transmissions are similar. WiFiNet APs also compute σ^2, by measuring the variance in the received power values (Figure 8 (right)). Knowing μ_{il}, σ and $\hat{r}_i$, the controller can compute $P(\hat{r}_i|l)$ using,

$$P(\hat{r}_i|l) = \frac{1}{\sigma\sqrt{2\pi}} e^{-(\hat{r}_i - \mu_{il})^2/2\sigma^2} \quad (4)$$

Intuitively, each AP_i propagates a probability that is maximum around a circle with center at grid i and radius equal to μ_{il}. If the transmit power R^o of the device is known, plugging in $P(\hat{r}_i|l)$ in Equation 3 and iterating over all the grids and APs, we can compute the grid l with the maximum probability of finding the device.

Case of unknown transmit power (Model-UTP). If R^o is not known, we can factor it out by considering each pair of APs: if the non-WiFi device is at a grid l, the *expected difference* in the mean received powers at AP_i and AP_j can be modeled as $\lambda(i,j,l) = \mu_{il} - \mu_{jl} = 10\gamma log_{10}(d_{jl}/d_{il})$, and expected difference in the powers follows a normal distribution with twice the variance: $\mathcal{N}(\lambda(i,j,l), 2\sigma^2)$ [6]. Now, knowing $(\hat{r}_i - \hat{r}_j)$, we can compute $P((\hat{r}_i - \hat{r}_j)|l)$ as

$$P(\hat{r}_i, \hat{r}_j|l) = \frac{1}{2\sigma\sqrt{2\pi}} e^{-(\hat{r}_i - \hat{r}_j - \lambda(i,j,l))^2/4\sigma^2} \quad (5)$$

and we can localize the non-WiFi device by finding

$$\text{argmax}_l \sum_{i,j} \log P\big((\hat{r}_i - \hat{r}_j)|l\big) \quad (6)$$

i.e., each AP pair propagates a probability $P((\hat{r}_i - \hat{r}_j)|l)$ on every grid l. The probabilities are high for the grids where the difference in received powers $(\hat{r}_i - \hat{r}_j)$ is close to $(\mu_{il} - \mu_{jl})$. After processing all AP pairs, the algorithm outputs the grid l with the maximum probability.

— *Example.* Figure 9 (top, left) shows a deployment of 8 APs along with the location of an FHSS cordless phone (shown using a star). The rest of the figures show how the grid probabilities indicating the location of the phone change after processing 1, 6 and all possible AP pairs.

2.4.2 Alternative localization methods

We also implemented several other localization schemes ranging from simple methods such as (i) *Strongest-AP*, picking the AP with the strongest received power as the device's location, and (ii) *Centroid*, picking the centroid of three APs with the strongest received powers, to more sophisticated approaches like (iii) an *Iterative* approach that performs an exhaustive search over all parameters (γ, σ, R^o, l) to find the grid l with the maximum probability, and (iv) a *Fingerprinting* approach where we profile the environment using *WiFi transmissions* — we transmitted WiFi packets using a laptop placed at several locations, and at each location WiFiNet APs measured the signal strength to derive the RSS vector. We then *normalize* the vectors to nullify the effect of a the transmit power of the laptop and derive a location's *fingerprint*. Localization is performed by measuring the RSS vector (after normalization) of a non-WiFi device and finding the fingerprint that is the closest match. In §3, we compare our model based localization algorithms to all the above methods.

3 Experimental Results

The goal of our evaluation is to systematically benchmark WiFiNet's performance in diverse scenarios, and demonstrate its utility in realistic network settings. We break our evaluation into four parts: First, we demonstrate WiFiNet's ability in accurately characterizing the impact of different non-WiFi devices in a variety of scenarios. Second, we evaluate WiFiNet's accuracy in physically locating the non-WiFi interferers. Third, we emulate a non-WiFi interference prone enterprise WLAN scenario and show WiFiNet's utility in such a setting. Fourth, we benchmark different components of WiFiNet and highlight cases where WiFiNet's performance could degrade. We

start by presenting the details of our implementation.

Implementation. We implemented WiFiNet using commodity WiFi APs equipped with Atheros AR9280 wireless cards that are connected to a central controller (Linux PC with 3.33 GHz dual core Pentium IV, 4 GB DRAM) over the Ethernet. Our implementation consists of few hundred lines of C code and 9800 lines of Python scripts that implement non-WiFi device detection functionality at the APs [16], perform synchronization across multiple APs, and implement clustering algorithms, interference analysis and device localization methods at the controller.

Evaluation set up. We experiment with devices in 2.4 GHz spectrum, and our current prototype has been tested with 5 different non-WiFi devices types : (i) high duty devices (analog cordless phones), (ii) fixed-frequency pulsed transmitters (ZigBee devices), (iii, iv) two types of frequency hopping devices (FHSS cordless phones, Bluetooth devices), and (v) broadband interferers (microwave ovens). We run our experiments on two different deployments: (i) Deployment 1 used 8 APs (Figure 9) and (ii) Deployment 2 used 4 APs (Figure 20). We experiment with different non-WiFi device locations, 802.11 rates, channel conditions and traffic patterns: (i) UDP with saturated traffic as well as reduced traffic loads, and (ii) replay of real HTTP/TCP wireless traces (§3.1.6). Unless otherwise stated, we run WiFi links on 802.11 rate to 6 Mbps and use backlogged UDP traffic with a packet size of 1400B.

Ground truth. The conventional approach for measuring interference between WiFi links is to use bandwidth tests [20, 11] to determine the ground truth about the impact of a WiFi interferer on a WiFi link. We follow a similar approach to determine the impact of a non-WiFi interferer on a WiFi link: we perform controlled experiments where we send backlogged traffic on the WiFi link and (i) measure $p[L]$, the loss rate when the interferer is inactive, and (ii) measure $p[I \cup L]$, the loss rate when the interferer is active. However, unlike WiFi bandwidth tests wherein both the interferer and the link are using backlogged traffic and are active for the entire duration, a non-WiFi interferer may not be active all the time, leading to the case where $p[O]$ may be less than 1. For example, while high duty devices like analog cordless phones have $p[O] = 1$, other devices like FHSS cordless phones may only hop onto the WiFi channel of interest for a particular duration (when the WiFi link is backlogged, it turns out that $p[O] = 0.28$ for an FHSS cordless phone), or devices like microwave ovens have a characteristic duty cycle of 50% (*i.e.*, $p[O] = 0.5$). Therefore, impact given overlap, $p[I|O]$ has to computed as follows. $p[I \cup L]$ can be expressed as $p[(I \cup L)|O] \cdot p[O] + p[(I \cup L)|\neg O] \cdot p[\neg O]$. Now, $p[(I \cup L)|\neg O]$ is equal to $p[L]$, and expanding $p[(I \cup L)|O]$ in terms of $p[I|O]$ and $p[L]$, followed by a bit of algebra gives us

$$p^{\text{Actual}} = p[I|O] = \frac{\Big(p[I \cup L] - p[L]\Big)}{\Big((1 - p[L]) \cdot p[O]\Big)} \qquad (7)$$

Using controlled experiments, we measure $p[L]$ (loss under isolation) and $p[I \cup L]$ (loss when the non-WiFi device is active). Now, knowing $p[O]$, we can measure $p[I|O]$ and subsequently compute the overall impact, $p[I]$. For experiments involving multiple devices, we measure the ground truth by activating only one device at a time and measuring its impact on the link. We note that the same ground truth ($p[I|O]$) is valid when multiple devices are activated simultaneously (the overall impact $p[I]$ may change, but $p[I|O]$ remains the same). WiFiNet, however, computes $p[I|O]$ estimates in presence of multiple, simultaneously active devices and WiFi links using any traffic load.

We further note that controlled experiments such as bandwidth tests require high overhead to compute the interference estimates for all links in the network. In operational networks, doing so may not be possible as such an approach requires network downtime where all the other WiFi links (and non-WiFi interferers) have to be silenced [20]. WiFiNet, on the other hand does not place any such requirements (e.g., backlogged traffic on links or network downtime), and can compute the estimates in real-time by passively accumulating frame and pulse transmission information.

Metrics used. For interference estimation, we compare WiFiNet's real-time, passive interference estimate of "impact given overlap" ($p[I|O]$) with that obtained using controlled experiments wherein the device is activated in isolation (ground truth). For localization, we report the difference in the actual and the predicted location of the non-WiFi device (*i.e.*, localization error) in meters.

3.1 Validating Interference Estimates

We start by validating WiFiNet's interference estimates across a variety of scenarios.

3.1.1 Single interferer scenarios

Method. We experiment with a total of 165 link-interferer scenarios comprising 4 non-WiFi devices — a microwave oven, an analog cordless phone, an FHSS cordless phone and a ZigBee transmitter. We activate each device in turn, and place it at different distances to vary the interference on the monitored WiFi link. We compute the ground truth (actual $p[I|O]$) using controlled experiments that measure the link loss rate when the device is active and that when the device is inactive. Next, we *randomly* activate and

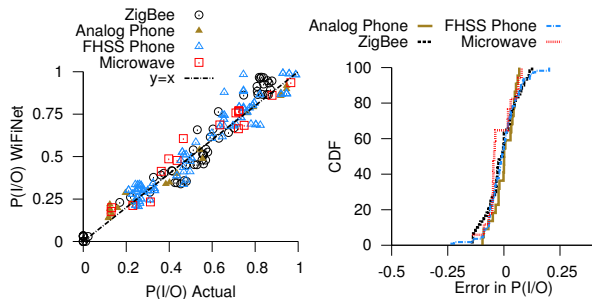

Figure 10: (left) Interference estimates obtained using controlled measurements (ground truth) and WiFiNet on 165 link-interferer scenarios comprising 4 different classes of devices. (right) CDF of error in interferer estimates is within ± 0.1 for 95% of the cases.

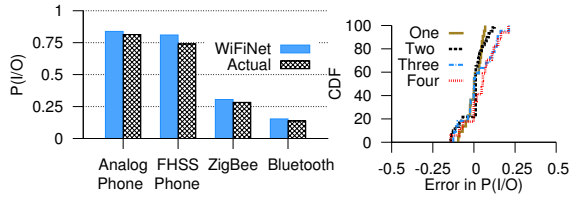

Figure 11: Accurately identifying impact of each interferer in the presence of multiple non-WiFi devices. (left) example scenario showing WiFiNet is able to identify the strong interferers (analog cordless phone, FHSS phone) and weak interferers (ZigBee and Bluetooth devices) accurately. (right) CDF of error in inteference estimates in the presence of multiple interferers.

de-activate the non-WiFi device while the WiFi link is active and measure WiFiNet's real-time estimate.

Results. Figure 10 (left) shows that WiFiNet correctly estimates a non-WiFi device's impact — across all device types and different amounts of interference (ranging from weak to strong), WiFiNet's estimates lie close to the ground truth (the points lie close to $y = x$). Figure 10 (right) shows that the overall error in WiFiNet's estimate is within ± 0.1 for more than 95% of the cases for all 4 devices.

3.1.2 Multiple interferers of different types

Method. In each run, we choose upto 4 random devices of different types, place them at random locations, randomly activate and de-activate them, creating scenarios when these devices are *simultaneously* active and measure WiFiNet's interference estimate for each device. For ground truth, we activate only one device at a time and perform controlled measurements. We repeat the experiments for different combinations of devices and locations.

Results. Figure 11 (left) shows a particular run which comprised two strong interferers (analog phone and FHSS cordless phone) and two weak interferers (ZigBee and Bluetooth devices). We find that WiFiNet is not only able to accurately identify the strong and weak inteferers, but is also able to discern the exact impact of each of these devices in spite of them being active simultaneously. Figure 11 (right) shows the CDF of error in interference estimates for combinations of 2, 3 and 4 devices across 60 runs. While the overall error slightly increases with increase in the number of devices, the error is within ± 0.15 for more than 85% of the cases even when operating 4 devices. The slight increase in error is due to increased overlap in the transmissions from multiple devices. We benchmark the effect of overlapping transmissions in §3.4.4.

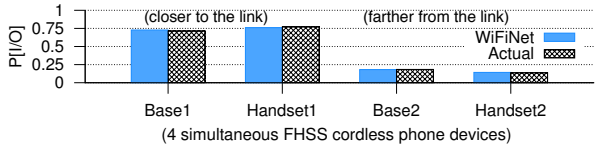

Figure 12: WiFiNet's accuracy in the presence of multiple non-WiFi devices of the same type. Out of 4 FHSS cordless phone devices, 2 are placed close to the link, and 2 are placed farther away.

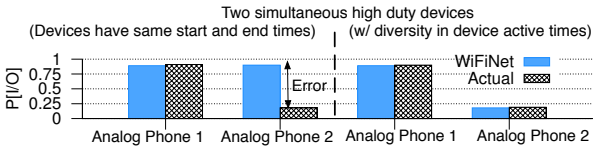

Figure 13: (left) Switching on and off 2 high duty devices (analog phones) *at the exact same time* causes WiFiNet to incorrectly identify the interferers. (right) Allowing diversity resolves the issue.

3.1.3 Multiple interferers of the same type

Method. We now evaluate WiFiNet's performance when simultaneously operating multiple devices of the *same type*. We use 4 FHSS cordless phone devices — one base/handset pair is placed close to the WiFi link (to create strong interference), whereas the other pair is placed farther away (to create weak interference).

Results. Figure 12 shows that WiFiNet is able to (i) accurately identify all 4 FHSS cordless phone devices using clustering mechanisms (benchmarked in §3.4.3) and (ii) accurately identify strong interferers (base/handset pair placed close to the link) and weak interferers (base/handset pair placed farther away from the link).

3.1.4 Case of multiple high duty devices

Method. We place an analog phone near the WiFi link (strong interferer) and another analog phone (operating at a frequency different from the first one), farther away from the WiFi link (weak interferer). We show results for two cases: (i) we switch activate and de-activate both the phones *at the exact same time*, and (ii) we activate the second phone 5 seconds after the first phone.

Results. Figure 13 (left) conveys that while WiFiNet is able to identify two different phones (by virtue of their different center frequencies), it incorrectly tags both the phones as strong interferers. Since both the analog phones are switched on and off at the *same time*, and they are high duty devices that are *always-on* (*i.e.*, they continuously emit energy), WiFiNet cannot distinguish between the in-

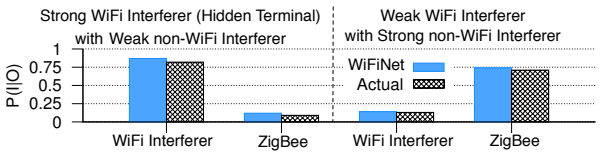

Figure 14: Estimating the interference impact of a WiFi interferer (hidden terminal) and a non-WiFi interferer (ZigBee device).

Figure 15: WiFiNet's ability to track the changing interference patterns for a client that is moving away from a ZigBee interferer. (left) instantaneous throughput at the client (right) delivery in isolation (*i.e.*, in absence of overlap), impact given overlap ($p[I|O]$) and actual impact ($p[I]$) are shown.

terference impact of the two devices. Figure13 (right) shows a more practical scenario where introducing a little diversity (*i.e.*, a lag of 5 secs in the device start times) allows WiFiNet to correctly estimate the interference.

3.1.5 Mix of WiFi and non-WiFi interference

Method. We evaluate WiFiNet's accuracy when simultaneously operating a WiFi interferer (hidden terminal) and a non-WiFi interferer (ZigBee device). The interferers are placed at different distances from the monitored WiFi link to create two scenarios: (i) strong WiFi interferer with a weak non-WiFi interferer (ii) weak WiFi interferer with a strong non-WiFi interferer. The WiFi interferer's traffic follows an http on-off model for with sleep and active times derived from a wireless trace [17], whereas the ZigBee device used a constant bit rate. As before, to measure ground truth, we operate the devices in isolation.

Results. Figure 14 shows the results. In case (i), WiFiNet finds that losses are more likely to happen when the monitored link's frames overlap with WiFi interferer's frames, whereas in case (ii), the losses show a high correlation when frames overlap with non-WiFi device's transmissions, resulting in accurate estimates for both cases.

3.1.6 Dynamic interference settings

Handling WiFi client mobility. We now evaluate WiFiNet's ability in updating the interference estimates that reflect the changing impact of a non-WiFi interferer due to client mobility. We use the set up shown in Figure 15 (top) where in a WiFi client is moving away from a ZigBee interferer. In the figure, plot on the left shows the instantaneous throughput at the client increases as

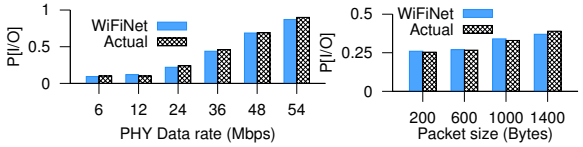

Figure 16: (i) Impact of PHY rate and (ii) packet size on $p[I|O]$ in presence of a ZigBee interferer. For (i), packet size is fixed at 1400 bytes, and for (ii), rate is fixed at 12 Mbps. $p[I|O]$ rises sharply with rate, the change in $p[I|O]$ with packet size is less pronounced.

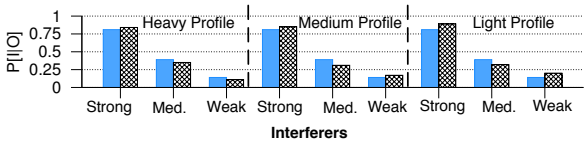

Figure 17: WiFi links replay real HTTP/TCP wireless traces (heavy, medium, and light profiles) in presence of strong, medium and weak interferers. WiFiNet's estimates closely match the ground truth in each case. The slight mismatch is due to the variability in packet sizes as the ground truth was measured using 1400 byte packets, whereas the traces comprised packets of different sizes.

it moves away from the interferer. The plot on the right shows WiFiNet's ability to track (i) delivery in isolation (*i.e.*, in the absence of overlap) that shows a slight increase, (ii) the impact given overlap $p[I|O]$, which rapidly drops down from 0.98 to 0.2 as the client moves farther away and (iii) the actual impact $p[I]$, owing to the probability of overlap, drops from 0.3 to 0.12. The decrease in the actual impact closely matches with the increase in throughput confirming WiFiNet's utility in understanding client performance in dynamic wireless environments.

Variable 802.11 rates and packet sizes. We evaluate WiFiNet's ability to dynamically track the changing interference estimates due to changes in (i) PHY rates and (ii) packet sizes used by the links. For ground truth, we perform controlled experiments at each PHY rate, whereas for WiFiNet we enable dynamic rate adaptation using SampleRate and capture the estimates in real-time. Figure 16 (left) shows that WiFiNet's estimates derived from rate adaptation closely match the ground truth. Since higher rates require higher SINR to decode a frame successfully, impact of the interferer *increases* with the increase in rate. Next, we fix the PHY rate (to 12 Mbps) and repeat our experiments for different packet sizes. Figure 16 (right) shows that WiFiNet is correctly able to track the slight increase in the interferer's impact at larger packet sizes.

Replay of wireless traces. We evaluate WiFiNet's performance using publicly available Sigcomm 2004 traffic traces [17]. We partitioned the trace into heavy, medium, and light periods corresponding to periods with airtime utilization of more than 50%, between $20-50\%$, and less than 20% respectively, at different times of the conference [20]. The HTTP/TCP sessions are then replayed on WiFi links (using the mechanism described in [7]) in the presence of strong, medium and weak ZigBee interfer-

Delay	Min.	25th %ile.	median	75th %ile	Max.
Convergence time	319 ms	549 ms	972 ms	1.7 sec	3.6 sec

Table 1: Distribution of convergence time for WiFi links replaying HTTP/TCP wireless traces (heavy, medium and light profiles) in presence of an FHSS cordless phone interferer.

Algorithm	Min. error	25th %ile.	median	75th %ile	Max error
Iterative	0.3m	0.8m	2.1m	4m	10m
Model-TP	0.3m	0.3m	1.3m	3m	8m
Model-UTP	0.3m	0.8m	1.3m	4m	11m

Table 2: Overall localization error for an analog cordless phone and an FHSS phone when placed at random locations in deployment 2.

ers. Each client emulated the behavior of one real client from the trace, faithfully imitating its HTTP transactions. Figure 17 shows that that WiFiNet's interference estimates are close to that of the ground truth across different traffic profiles and interfering scenarios. The slight differences between the estimates are due to the variability in packet sizes in the real traces, compared to the ground truth that was measured using 1400 byte packets. We also show the CDF of time taken by WiFiNet to converge to the right $p[I|O]$ estimates in Table 1 (median $<$ 1 sec). We benchmarks the factors affecting convergence time in §3.4.1.

3.2 Accuracy of Localization

We now evaluate our localization algorithms.

3.2.1 Accuracy across different classes of devices

Figure 18 shows CDF of localization error for two non-WiFi device types: (i) frequency-hopping cordless phone and (ii) high duty, analog cordless phone, when using deployment 1 with 8 APs shown in Figure 9. Devices were placed at random locations and for each location, we compute the difference in the predicted and actual location for 5 different localization schemes (§2.4). We find that all algorithms perform well, resulting in a median error of $1-3$ meters for the FHSS phone, and $1.7-4$ meters for the analog phone. Here, WiFiNet's modeling based localization approaches perform similar to the Iterative approach that employs an exhaustive search, and is better than Fingerprinting (§2.4.2) that incurs a profiling overhead. Accuracy of Fingerprinting, however, can be improved by increasing the density of fingerprints (0.05/sq.meter in this case) at the cost of a higher profiling overhead.

3.2.2 Effect of AP density

In each run, we randomly chose a subset of 4 APs (out of the 8 APs in deployment 1) and compute the localization error. We repeat the experiment for 25 runs and report the average error in Figure 19 (left). We observe that when the density of the AP deployment is sparse, the performance of Centroid algorithm worsens (median error of 8 meters) compared to the other algorithms (median error of 2.5 to 4.8 meters). Figure 19 (right) shows the degradation in the performance of Model-UTP, when the number of APs

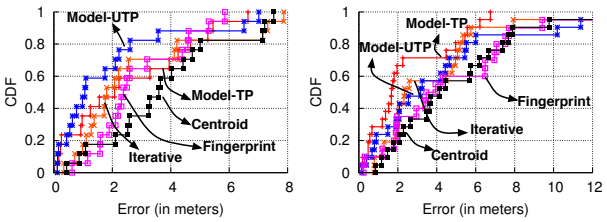

Figure 18: Accuracy of localization for (left) FHSS cordless phone and (right) analog cordless phone for deployment 1 (Figure. 9).

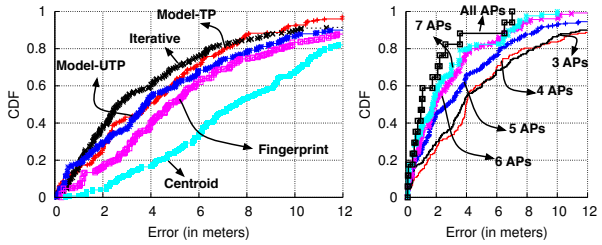

Figure 19: Localization accuracy for FHSS cordless phone (left) for subsets of 4 APs from deployment 1 (right) using Model-UTP when the number of APs was decreased from 8 to 3.

is reduced from 8 to 3. The median error only increases from 1 meter to 4 meters indicating the better performance of modeling based approaches in sparse deployments.

3.2.3 Improvements with fine-grained modeling

To understand the benefits from using a per-AP path loss exponent, we compare the performance of our modeling-based localization approaches when a uniform path loss exponent is used. Table 3 shows that when switching to a uniform path-loss exponent, the median error increased from 1.7 to 3.6 meters, and the maximum error increased from 6.7 meters to 12 meters. Using a per-AP path loss improves the WiFiNet's localization accuracy as it takes into account the differences in the environments surrounding the APs (e.g., walls and other obstacles).

3.2.4 Location insensitivity

We repeated our experiments to benchmark the performance of our algorithms in a different topology and environment (deployment 2 with 4 APs, Figure 20). Table 2 shows the overall error for the modeling-based and Iterative approaches. We find that the algorithms perform well with a median error of $1.3-2.1$ meters.

3.2.5 Impact of transmit power

Our experiments with localizing Bluetooth devices resulted in an increased median error ($2-6.7$ meters) — owing to its low transmit power, only one of the APs could detect the Bluetooth device. In this case, the WiFiNet resorts to the Strongest AP approach for localization (§2.4).

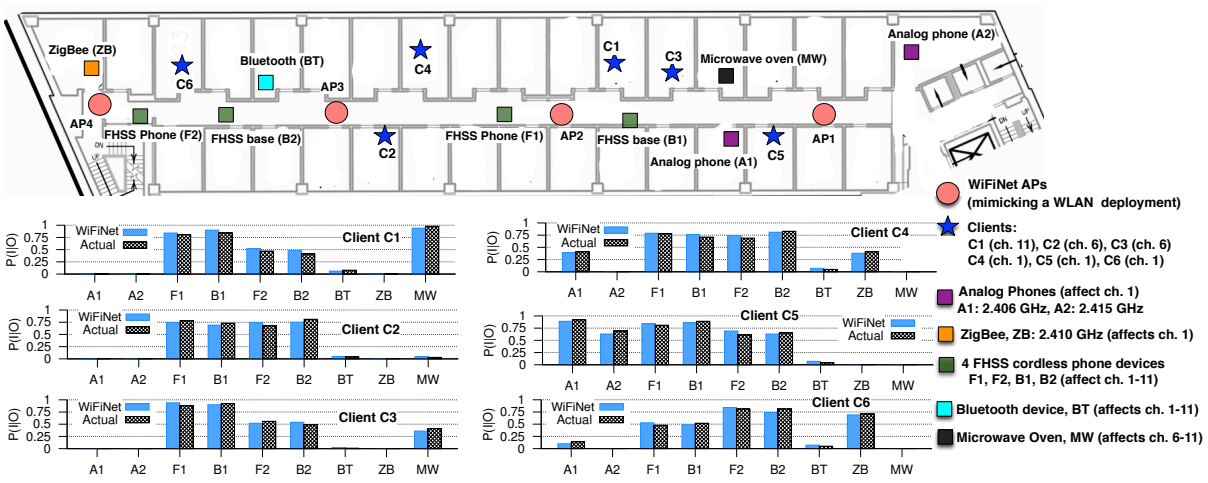

Figure 20: Emulating an enterprise WLAN with 4 APs and 6 clients. A total of 9 non-WiFi devices are placed to interfere with the clients: 2 analog phones, 4 FHSS cordless phone devices, a Bluetooth device, a ZigBee device and a microwave oven. WiFiNet is able to accurately characterize the interference impact ($p[I|O]$) of all devices (even those of the same type) on each of the clients.

Scheme	Min. error	25th %ile.	median	75th %ile	Max error
Uniform γ	0.2m	1.9m	3.6m	7m	12m
per-AP γ	0.2m	2.0m	1.7m	2.3m	6.7m

Table 3: Overall localization error for the Model-TP algorithm with (i) uniform and (ii) per-AP path loss exponents (deployment 1).

3.3 Emulating an Enterprise WLAN

We now try to emulate the structure of our in-building WLAN by placing a WiFiNet AP near each production AP and distribute clients into offices (Figure 20). Our topology consists of 4 APs and 6 clients. We use a total of 9 non-WiFi interferers: 2 analog phones (high duty devices), 4 FHSS cordless phone devices, a Bluetooth device (frequency hopping devices), a ZigBee device (fixed frequency, pulsed transmitter) and a microwave oven (broadband interferer). WiFi links are assigned channels (shown in Figure 20) so as to create a scenario where each non-WiFi device affects at least one link. Each WiFi link follows an HTTP traffic model, with on-off times derived from a wireless trace [17]. We activate and de-activate the non-WiFi devices randomly, creating scenarios when devices are simultaneously active. As before, for ground truth measurements, we activate only one device at a time.

Figure 20 shows the interference impact of each interferer on the WiFi links — depending on the channel of operation, location of the client, and overlap probability (based on the actual WiFi traffic and non-WiFi device activity), WiFi links experience different amount of interference from each non-WiFi device. Further, WiFiNet's estimate *closely matches* the ground truth for each case. We find that all 4 FHSS cordless phone devices affect *all* the WiFi links ($p[I|O]$ varied from 0.45 to 0.8 due to their high transmit power of -20 dBm). The overall impact $p[I]$, however, only varied from 0.1 to 0.31 owing to their frequency hopping nature. Peak emissions of microwave

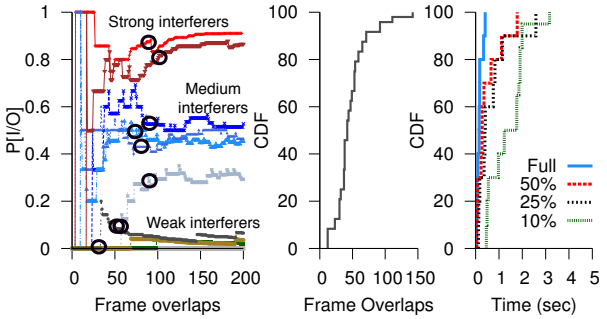

Figure 21: (left) Number of frame overlaps are required to converge for 10 ZigBee interferer scenarios including strong, medium and weak interference (middle) CDF of the number packet overlaps required for $p[I|O]$ to converge (right) Convergence time as a function of the traffic load for an FHSS cordless phone.

ovens are typically in 2.45 to 2.47 GHz, and so the oven severely affected the client $C1$ which operated on channel 11. It is interesting to note that $C3$ (operating on channel 6) was also affected by the oven ($p[I|O]$=0.36) as it was close to the device, whereas $C2$ (channel 6, farther from the device) and $C5$ (channel 1, closer to the device) were not affected. Bluetooth device, due to its low power and adaptive frequency hopping nature did not significantly affect any of the links. On the other hand, high powered and high duty device like analog phones (A1 and A2) affected the clients on channel 1 (C4, C5, C6) much more than the ZigBee device that had a lower transmit power.

3.4 Microbenchmarks and Other results

We now benchmark convergence time, clustering algorithms, highlight cases where WiFiNet can under perform, and present results on estimating sender-side interference.

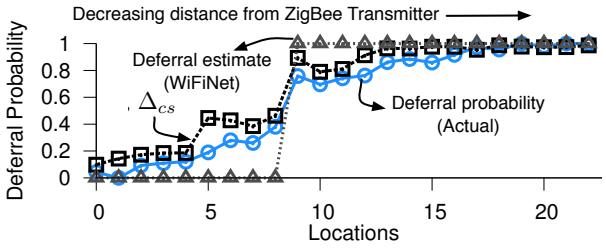

Figure 22: WiFiNet's estimates of deferral probability close match the ground truth. Here, a WiFi transmitter is moving toward a ZigBee interferer leading to increase in the deferral probability.

3.4.1 Convergence time

We define the convergence time as the time taken by WiFiNet to gather sufficient samples (*i.e.*, overlaps between WiFi frames and non-WiFi transmissions) to compute an accurate $p[I|O]$ estimate (within ± 0.1 of the ground truth). Figure 21 (left) shows 9 different scenarios where a ZigBee interferer causing strong, medium or weak interference is activated along with a WiFi link. Across all scenarios, we find that < 100 overlaps between WiFi frames and ZigBee transmissions are enough for $p[I|O]$ to converge (convergence points shown with black circles). Across different non-WiFi interferers and links < 150 overlaps are enough to converge to the ground truth (CDF shown in Figure 21 (middle)). The time for convergence depends on the WiFi link's traffic load, and the activity of the non-WiFi device. Figure 21 (right) shows that although the convergence time increases with lesser traffic, it is less than 4 seconds across a variety of traffic loads when using an FHSS cordless phone as an interferer. For devices like microwave ovens and analog cordless phones, convergence time was much lesser owing to increased overlaps.

3.4.2 Estimating sender-side interference

We also benchmarked WiFiNet's ability to correctly estimate the carrier sensing interference across a number of non-WiFi devices and links. Here, we move a WiFi transmitter toward a ZigBee device (periodically transmits 4 ms pulses) and measure its deferral probability (§2.3). For ground truth, we measure the transmitter's sending rate when the device is active and that when the device is inactive. WiFiNet estimates the deferral probability in real-time — we observe that Δ_{cs} *i.e.*, the fraction of Case (2) instances (§2.3) increases as we move the transmitter away, indicating increased deferral. Further, Δ_{cs} also closesly matches the ground truth deferral probability.

3.4.3 Performance of clustering

Clustering is straightforward in many cases e.g., when the devices are of different types, or in the case of fixed-frequency devices (of the same type) using different center frequencies. We benchmarked our RSS and timing based clustering algorithms (§2.2) for the harder cases of (i) fixed-frequency devices using the same center frequency and (ii) frequency hopping devices. Table 4 shows the overall summary (when operating up to 4 devices of the same type). We find that clustering algorithms perform reasonably well with $> 88\%$ accuracy in detecting the number of device instances. In case of over-clustering, the number of pulses in the extra clusters were relatively low, allowing us to discard the false positives. Under-clustering, however, can lead to error in estimates that can happen if the devices are close to each other (§3.4.4). Using timing attributes (when available) results in increased accuracy, compared to RSS based clustering, as timing attributes are not sensitive to the distance between devices (§3.4.4). Also, k-means+EM clustering has higher accuracy compared to density based clustering (DBSCAN).

Algorithm	Attribute	Clustering performance		
		% Correct	% Over-cluster	% Under-cluster
DBSCAN	Timing	92.7%	5%	2.3%
DBSCAN	RSS	88.7%	5.2%	6.1%
k-Means + EM	Timing	97.6%	1.3%	1.1%
k-Means + EM	RSS	91.4%	6.5%	2.1%

Table 4: Performance of clustering mechansisms used in WiFiNet. Results for two clustering algorithms (DBSCAN and k-means+EM) using (i) start time offset and (ii) RSS attributes are shown. Up to non-WiFi devices of the same type were placed at random locations.

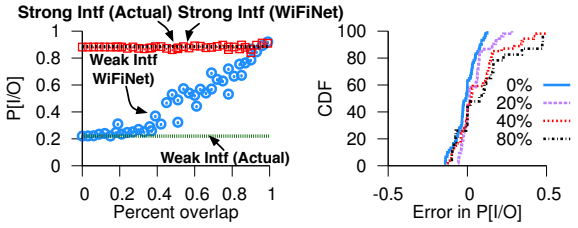

Figure 23: (left) Ability of WiFiNet to correctly identify interferers when transmissions from two non-WiFi devices overlap. $p[I|O]$ measured by WiFiNet for both strong ($p[I|O] = 0.88$) and weak ($p[I|O] = 0.22$) interferers as a function of their overlap in transmission times. If the overlap is less than 45%, WiFiNet can distinguish the strong and weak interferers accurately. (right) Ability of WiFiNet to correctly estimate $p[I|O]$ of an interferer as function of percentage of pulses lost (*i.e.*, not captured) by an WiFiNet AP.

3.4.4 Sources of error

We now highlight some of the scenarios where WiFiNet's performance can degrade.

Overlapping transmissions. We now benchmark the effect of transmission overlaps between multiple interferers. Figure 23 (left) shows WiFiNet's interference estimates in the presence of a strong and a weak non-WiFi interferer, as a function of the overlap between their transmission times. In the unlikely case when the transmissions from both non-WiFi devices overlap 100% of the time, WiFiNet is unable to distinguish between the two. However, as the percentage of overlap decreases, WiFiNet is able to discern the impact of the weak interferer. In practice, we expect diversity in device transmission times [16] to allow WiFiNet to output accurate interference estimates.

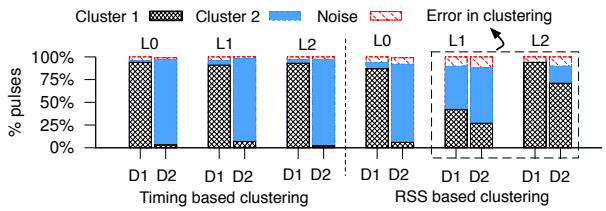

Figure 24: Performance of clustering for 2 FHSS cordless phone devices as a function of the distance between them. Clustering using (i) timing properties is unaffected by the distance, whereas that using (ii) RSS performs incorrect clustering when the devices are placed ≤ 5 meters apart (L1, L2). For L0, devices were 10 m apart.

Coverage. WiFiNet's ability to derive an accurate interference estimate depends on how well the non-WiFi device's transmission are captured. In particular, $p[I|O]$ and $p[L]$ estimates will differ from the ground truth when none of the WiFiNet APs capture the device's transmissions. Figure 23 (right) shows the impact of losing transmissions from non-WiFi interferers — the error in estimates increase with decrease in the percentage of captured transmissions. In a typical enterprise deployment with multiple APs, this might not be a concern as we can expect at least one AP to capture the device's transmissions.

Proximity between devices. We now present a case when clustering mechanisms can under perform. We experiment with 2 FHSS cordless phone devices and place them at different distances. Figure 24 shows that timing based clustering is unaffected by the distance between the devices, but RSS based clustering is not. When the devices are placed ≤ 5 meters apart (at L1, L2), RSS based clustering cannot distinguish them as their RSS vectors look similar. This results in under-clustering (pulses of both devices are put into one cluster) or incorrect clustering (each cluster has a mixture of pulses from both devices).

4 Related Work

We now present the related work in the areas of non-WiFi device interference estimation and localization.

Device detection and interference estimation. Commercial solutions such as Wispy [4], Cisco Spectrum Expert [2] and Bandspeed AirMaestro [1] use custom hardware (signal analyzer ICs) to detect RF devices operating in the medium. However, these solutions do not provide the capability to estimate the interference caused by the non-WiFi devices to the the WiFi links. Recent research work such as DOF [8], RFDump [13], TIMO [18] can also detect the presence of non-WiFi device activity using specialized hardware such as channel sounders and software-defined radios. Such platforms enable TIMO and DOF to go beyond detection and employ signal processing techniques to mitigate interference and develop mechanisms to co-exist with non-WiFi devices. WiFiNet takes a step towards empowering APs and clients with such functionality, by providing non-WiFi interference estimation capability under the constraints of commodity WiFi hardware. In [14], the authors use a single WiFi card to infer interference from Bluetooth and microwave ovens by analyzing the timing of WiFi packet errors. However, their technique does not generalize to detect inteference other non-WiFi devices that don't exhibit timing properties (e.g., ZigBee) and cannot distinguish between devices of same type. In comparison, WiFiNet can also estimate the interference from multiple, simultaneously operating devices and pin-point their location in the physical space.

Device localization. There has been limited prior work on designing a generic system to localize the various non-WiFi devices on the top of commodity WiFi hardware. Existing literature has looked at localizing specific device types (e.g., Bluetooth [19], Zigbee [9]) by using sensors of the same type. Amongst commercial solutions, Wi-Spy device finder [4] uses a directional antenna and requires a user to walk and manually search for the location of the transmitter. Cisco CleanAir [2] finds the location of RF transmitter sources by using specialized hardware in the access points. WiFiNet uses only commodity WiFi cards to not only detect the location of non-WiFi devices, but also estimate their interference impact.

5 Conclusion

We presented WiFiNet, a system to estimate the interference experienced by WiFi links in presence of non-WiFi devices using only WiFi hardware. WiFiNet can correctly estimate the impact of each non-WiFi device, in presence of multiple other interferers, even if they are of the same type. It also correctly tracks changes due to client mobility, dynamic traffic loads, and varying channel conditions. Further, WiFiNet also identifies the physical locations of non-WiFi devices. We believe a system such as WiFiNet can help WLAN administrators use commodity WiFi APs to better understand and manage non-WiFi interference, especially in environments such as enterprise WLANs.

References

[1] Bandspeed AirMaestro. http://www.bandspeed.com/.
[2] Cisco Spectrum Expert. http://tinyurl.com/5eja7f.
[3] The WEKA data mining software: an update. ACM SIGKDD Explorations Newsletter.
[4] Wi-Spy spectrum analyzer and device finder. www.metageek.net.
[5] P. Bahl and V. N. Padmanabhan. Radar: an in-building rf-based user location and tracking system. In *Infocom'00*.
[6] B.Lin and J. Wu. Analysis of hyperbolic and circular positioning algorithms using stationary signal-strength-difference measurements in wireless communications. In *VTC*, 2003.
[7] J. Eriksson, S. Agarwal, P. Bahl, and J. Padhye. Feasibility study of mesh networks for all-wireless offices. In *MobiSys*, 2006.
[8] S. Hong and S. Katti. DOF: A local wireless information plane. In *ACM SIGCOMM 2011*.
[9] J. Blumenthal et. al. Weighted centroid localization in zigbee-based sensor networks. *IEEE ISISP'07*.
[10] J. Han and M. Kamber. Data Mining: Concepts and Techniques.
[11] J. Padhye et al. Estimation of link interference in static multi-hop wireless networks. In *IMC'05*.
[12] J. Sander et. al. Density-based clustering in spatial databases. *Data Mining Knowledge Discovery'98*.
[13] K. Lakshminarayanan et. al. RFDump: an architecture for monitoring the wireless ether. In *CoNext'09*.

[14] K. Lakshminarayanan et. al. Understanding 802.11 performance in heterogeneous environments. HomeNets '11.
[15] R. Mahajan et. al. Analyzing the mac-level behavior of wireless networks in the wild. *SIGCOMM '06*.
[16] S. Rayanchu, A. Patro, and S. Banerjee. Airshark: Detecting non-WiFi devices using commodity WiFi hardware. In *ACM IMC'11*.
[17] M. Rodrig, C. Reis, R. Mahajan, D. Wetherall, J. Zahorjan, and E. Lazowska. CRAWDAD data set uw/sigcomm2004.
[18] S. Gollakota et al. Clearing the RF Smog: Making 802.11 Robust to Cross-Technology Interference. In *ACM SIGCOMM 2011*.
[19] S. Thongthammachart and H. Olesen. Bluetooth enables in-door mobile location services. *VTC'03*.
[20] V. Shrivastava et. al. PIE in the Sky: online passive interference estimation for enterprise wlans. In *NSDI'11*.
[21] Y. Cheng et. al. Jigsaw: Solving the puzzle of enterprise 802.11 analysis. In *SIGCOMM'06*.
[22] M. Youssef and A. Agrawala. The horus wlan location determination system. In *MobiSys'05*.